

# PMMA-SiO<sub>2</sub> organic–inorganic hybrid films: determination of dielectric characteristics

M. D. Morales-Acosta · M. A. Quevedo-López ·  
Bruce E. Gnade · R. Ramírez-Bon

Received: 22 July 2010 / Accepted: 13 December 2010 / Published online: 6 January 2011  
© Springer Science+Business Media, LLC 2011

**Abstract** Organic–inorganic hybrid thin films have been prepared by a modified sol–gel route using tetraethyl orthosilicate as the inorganic (silica) source, methyl methacrylate (MMA) as the organic source, and 3-trimetoxypropyl methacrylate as the coupling agent. The films were prepared by spin coating on Si (100) p-type substrates and subsequently heat-treated at 90 °C. Fourier transform infrared results reveal a set of absorption bands associated with the formation of both PMMA and SiO<sub>2</sub> phases in the hybrid films. Capacitance–voltage (*C–V*) characterization was carried out on metal–insulator–metal (MIM) and metal–insulator–semiconductor (MIS) structures, with the hybrid films as the insulator layer to evaluate the electrical properties. We present a detailed comparative analysis of the dielectric constant obtained from *C–V* characterization in the frequency range of 1 kHz–1 MHz. For the PMMA-SiO<sub>2</sub> hybrid material the dielectric constant values obtained were around 9.5 at 1 MHz which is superior to the values reported for thermally grown SiO<sub>2</sub> and pure PMMA materials. The interface state density for PMMA-SiO<sub>2</sub> on Si was approximately 10<sup>10</sup> cm<sup>-2</sup>, which is comparable to the standard SiO<sub>2</sub>/Si structures. Due to the electrical behavior and low processing temperatures this hybrid dielectric is a very promising candidate for flexible electronic devices and its subsequent implementation does not require complex equipment.

**Keywords** Hybrid PMMA-SiO<sub>2</sub> · Organic–inorganic materials · Hybrid gate dielectric · Electrical properties · Dielectric characterization

## 1 Introduction

A great deal of research in the microelectronics industry has been on the improvement of materials. Much of this effort has been focused on improving the performance of the gate dielectric. During the last four decades SiO<sub>2</sub> has been the primary gate dielectric because it offers superior performance and key advantages in microelectronics processing, including a high quality and thermodynamically stable Si-SiO<sub>2</sub> interface as well as superior electrical isolation properties [1]. Recently, there has been an increasing interest in organic-based electronics for low cost and large area processability. The replacement of rigid substrates with flexible polymeric substrates requires novel dielectrics, semiconductors and contacts materials with good mechanical flexibility, low processing temperatures and acceptable performance. For flexible electronics, poly (methyl methacrylate) (PMMA) has been assessed as an option for the gate dielectric due to its high resistivity, chemical resistance, thermal stability, mechanical flexibility, low cost and dielectric constant similar to SiO<sub>2</sub> [2].

Organic–inorganic hybrid materials, have received much attention due to their unique and novel properties that can be achieved from blending properly the organic and inorganic components. The PMMA-SiO<sub>2</sub> hybrid system has been synthesized using the sol–gel method [3, 4]. The sol–gel process is one of the most convenient methods to achieve the proper linking between the organic and inorganic phases at the molecular scale. Furthermore, the sol–gel route is suitable to produce multi-functional hybrid

M. D. Morales-Acosta · R. Ramírez-Bon (✉)  
Centro de Investigación y de Estudios Avanzados del IPN,  
Unidad Querétaro, Apdo. Postal 1-798, 76001 Querétaro,  
Qro, México  
e-mail: rrbon@qro.cinvestav.mx

M. A. Quevedo-López · B. E. Gnade  
Department of Materials Science and Engineering,  
The University of Texas at Dallas, Richardson, TX 75083, USA

inorganic–organic materials with properties that are difficult to attain using conventional methods [5]. In addition, using the sol–gel process the properties of the resulting hybrid PMMA-SiO<sub>2</sub> system can be tailored by choosing the appropriate compositions of the organic and inorganic starting phases. In this hybrid system the PMMA organic component provides large area substrate compatibility and flexibility at low processing temperature while the SiO<sub>2</sub> component improves the dielectric characteristics of the resulting hybrid material. These properties have prompted further studies of PMMA-SiO<sub>2</sub> as an alternate gate dielectric material. We believe this system can produce a new hybrid material with the required flexibility, dielectric properties and adherence to either rigid or flexible substrates at low processing temperature.

The understanding of the electrical behavior presents a challenge for any alternative gate dielectric candidate. Metal-insulator-metal (MIM) and metal-insulator-semiconductor (MIS) devices are structures widely used to characterize suitable gate dielectrics on a semiconductor. Electrical methods are used to extract the dielectric properties of the insulator and to determine the quality of the insulator/semiconductor interface. Here, we present a study of the electrical properties of PMMA-SiO<sub>2</sub> dielectric films deposited using a modified sol–gel route. The resulting hybrid thin films were evaluated as gate dielectric using MIM and MIS structures. Electrical properties of the PMMA-SiO<sub>2</sub> hybrid system were studied using current–voltage (*I*–*V*) and capacitance–voltage (*C*–*V*) in the 1 kHz–1 MHz frequency range.

## 2 Experimental details

The sol–gel method to prepare hybrid PMMA-SiO<sub>2</sub> films has been described in several publications [6, 7]. In this work, tetraethyl orthosilicate (TEOS) was used as the inorganic precursor and methyl methacrylate (MMA) as the source of the organic component. The use of a silane-based coupling agent, 3-trimethoxysilylpropyl methacrylate (TMSPM), improves the compatibility of the organic and inorganic phases. MMA polymerization was initiated with benzoyl peroxide (BPO). Ethyl alcohol was used as the organic solvent and water was used to hydrolyze the inorganic precursor. The molar ratio used was TEOS:TMSPM:MMA (1.0:0.15:1.0). The resulting homogeneous solution was spin-coated on clean substrates (the cleaning process is described below). Additionally, these samples were baked for 6 h in a conventional oven at 90 °C and atmospheric pressure.

The surface morphology of the hybrid PMMA-SiO<sub>2</sub> films was studied employing an Atomic Force Microscopy (AFM). The equipment used for this study was a

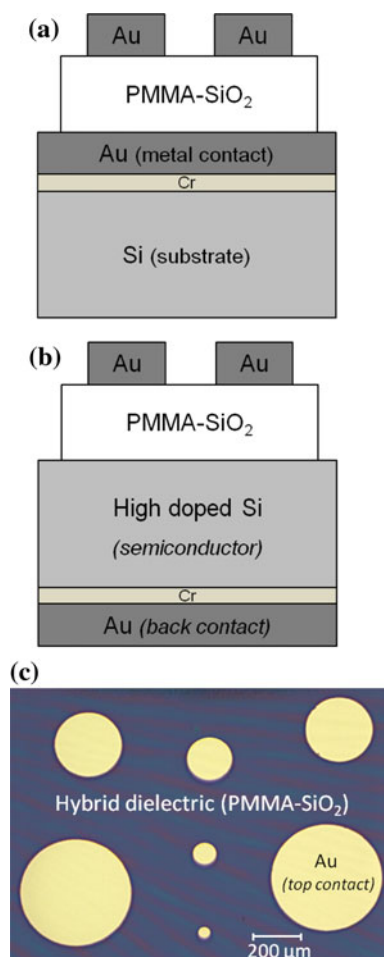
multimode microscope controlled by Nanoscope V electronics (Veeco Instruments Inc.) used in tapping mode, which was mainly used for roughness measurements and imaging of surface structure. Fourier transform infrared (FTIR) analyses of the PMMA-SiO<sub>2</sub> and its precursor materials was conducted using a Nicolet 6700 spectrometer in the Grazing Angle Attenuated Total Reflectance (GA-ATR) mode with a resolution of 4 cm<sup>-1</sup>, in the wave number range of 700–4,000 cm<sup>-1</sup>. Cross sectional SEM of the hybrid dielectric film was carried out in a Zeiss Supra-40 scanning electron microscope (SEM) operated at 10 kV to determine the dielectric thickness.

Electrical characterization (*C*–*V* and *I*–*V*) was performed on MIM and MIS structures fabricated using p-type Si (100) with a resistivity of 1–20 Ω cm. Prior to deposition, the silicon wafer substrates were cleaned with the RCA standard procedure and immersed in HF to remove the native SiO<sub>2</sub> from the surface. Gold films (100 nm) for the electrodes were thermally evaporated using a shadow mask to define top circular contacts (50, 100, 200, 300 and 500 μm diameter). All sample preparation steps were performed under clean room environment (US-class 10,000). Electrical characteristics were measured using a parameter analyzer (Keithley 4200) and a *C*–*V* analyzer (HP4284A, Hewlett Packard). Low and high frequency *C*–*V* data (from 1 kHz to 1 MHz) were acquired. Figure 1a depicts a graphic overview of the MIM gate structure used for *C*–*V* measurements. Figure 1b shows the MIS structure used for *C*–*V* and *I*–*V* characterization; and Fig. 1c top view (optical microscope image).

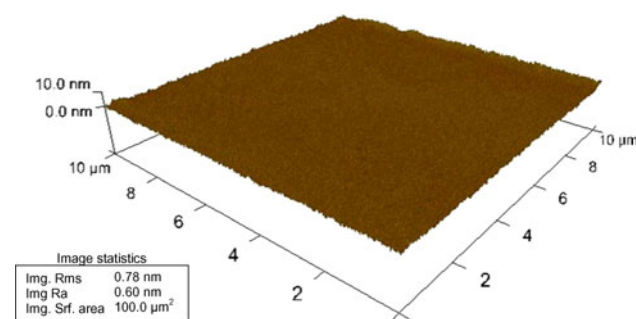
## 3 Results and discussion

Figure 2 is an AFM 3D image displaying the surface morphology in an area of 10 × 10 μm<sup>2</sup> of the PMMA-SiO<sub>2</sub> film. It is included in the figure the roughness statistics measured in this image. As can be observed, the surface of the hybrid film at microscopic level is uniform, flat and very smooth. The root mean square (rms) roughness of the film measured in this area is 0.78 nm which is a very low surface roughness value. There are not evidences of separate phase precipitation at this micrometric scale. Thus, the surface morphology of the hybrid film confirms the formation of a homogeneous mixed organic–inorganic material with very small domains in the nanometric scale.

Figure 3 shows the ATR-FTIR spectra of the PMMA-SiO<sub>2</sub> inorganic–organic hybrid material and for comparison those of the organic (PMMA) and inorganic (TEOS) contributions, and of the coupling agent (TMSPM) between both phases. The spectrum of PMMA material is the result of the polymerization of MMA by addition of BPO. The presence of the characteristics PMMA and SiO<sub>2</sub> absorption



**Fig. 1** **a** Schematic cross section of MIM structures, **b** MIS configuration and **c** Optical microscope image of the fabricated MIS devices (*top view*). Gold contacts were thermally evaporated through a shadow mask on spin-coated PMMA-SiO<sub>2</sub> hybrid dielectric film. The diameters of the top contacts are 500, 300, 200, 100 and 50 μm



**Fig. 2** Three dimensional AFM topography of the hybrid PMMA-SiO<sub>2</sub> films

bands in the PMMA-SiO<sub>2</sub> spectrum shows the hybrid nature of the synthesized material from the sol gel process. The band corresponding to the Si–O–Si symmetric mode is identified near 800 cm<sup>-1</sup> [8]. The vibrational mode related to the Si–OH group is observed at 940 cm<sup>-1</sup> [8], which is

attributed to un-reacted Si–OH groups from the condensation stage. The strongest absorption band detected between 1,300 and 700 cm<sup>-1</sup> is associated mainly with the inorganic contribution. The inset shows the deconvolution for the 1,000–1,250 cm<sup>-1</sup> region. The bands positioned at 1,060 and 1,200 cm<sup>-1</sup> have been assigned to the anti-symmetric stretching vibrations of Si–O–Si bonds in the transverse optical (TO) and longitudinal optical (LO) modes respectively [8]. The deconvoluted bands attributed to Si–O–C at 1,110 cm<sup>-1</sup> and C–O–C at 1,145 cm<sup>-1</sup> are also observed [6]. The absorption bands detected in the range from 1,290–1,480 cm<sup>-1</sup> and 2,810–3,000 cm<sup>-1</sup> are related with C–H contributions. The absorption peaks detected around 1,600 cm<sup>-1</sup> are due to organic contribution: C=C and C=O centered at 1,630 and 1,690 cm<sup>-1</sup>, respectively [9]. The wide band centered at 3,350 cm<sup>-1</sup> is attributed to O–H stretching modes [8], which are mainly due to Si–OH groups, but can also be a result of contributions from residual ethanol and molecular water adsorbed or from the hydrolysis of TEOS and TMSPM in the sol–gel process [10, 11]. Similar FTIR bands attributed to the organic and inorganic phases have been reported for describing the formation of hybrid materials of the type organic–inorganic containing silica [12–14]. Typical values of electronic polarizability, which contribute to the dielectric constant of the system, for the organic bonds contained in the PMMA-SiO<sub>2</sub> hybrid material, determined from the FTIR analysis, are summarized in Table 1 [15]. The data in this table indicate that C=O and C=C bonds have high polarizability.

The dielectric constant values ( $\kappa_i$ ) of the hybrid films were determined using the Eq. (1) for a parallel plate capacitor, where  $\epsilon_0$  is the permittivity of free space,  $A$  is the area of the capacitor and  $C$  is the measured capacitance [16].

$$\kappa_i = \frac{C}{\epsilon_0} \cdot \frac{t}{A} \quad (1)$$

The thickness of the PMMA-SiO<sub>2</sub> film ( $t$ ) was determined from cross sectional SEM images (Fig. 4). For PMMA-SiO<sub>2</sub> deposited on gold or silicon the average thickness was 440 nm. No organic–inorganic phase separation was observed.

For the  $C$ – $V$  characterization using MIM devices, the dielectric constant values of the hybrid film were determined from the constant capacitance values from the  $C$ – $V$  measurements at several frequencies in the voltage range from –20 to +20 volts (not shown). Results for capacitance density and dielectric constant of these devices are summarized in Figs. 5 and 6. The dielectric constant determined from these measurements is in the range 9–20 in the frequency range from 1 to 1,000 kHz. The  $C$ – $V$  characteristics of the MIS structures are presented in Fig. 7. MIS

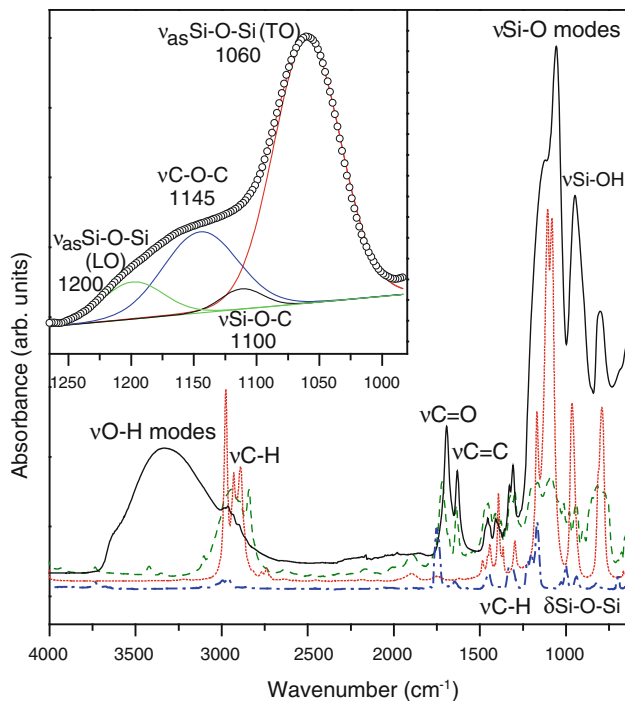


**Fig. 3** FTIR absorption spectra of TEOS (dotted line), PMMA (dashed-dotted line), TMSPM (dashed line) and PMMA-SiO<sub>2</sub> hybrid (full line) films. In the insert, the deconvolution of the wavelength range 1,250–1,000 cm<sup>-1</sup> is showed for PMMA-SiO<sub>2</sub> hybrid film

**Table 1** Electronic polarizability of PMMA-SiO<sub>2</sub> bonds

Bond	Polarizability (Å)
C–C	0.531
C–O	0.584
C–H	0.652
O–H	0.706
C=O	1.020
C=C	2.036

capacitors show the typical behavior at low (1 kHz) and high (10–1,000 kHz) frequencies. The curves clearly exhibit the accumulation, depletion and inversion regimes. The increment of the capacitance measured depends on the ability of minority carriers (electrons in this case for p-type semiconductor) to follow the variation of the applied signal. This only occurs at low frequency C–V measurements, where the rates of recombination and generation of minority carriers can keep up with the small signal variation and thus lead charge exchange with the inversion layer in step with the measured signal. Unlike depletion and weak inversion, at strong inversion the incremental charge is no longer at the edge of the depletion region but at the semiconductor surface inversion layer, resulting in a large capacitance. Experimental reports show that for metal-SiO<sub>2</sub>-Si system the capacitance is most frequency dependent in the range

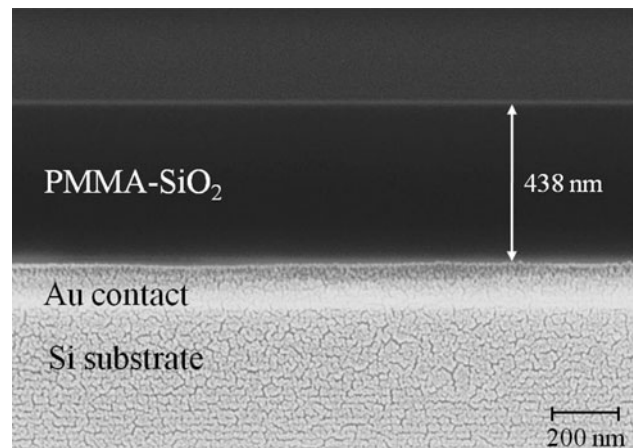


**Fig. 4** SEM micrograph of the cross section for PMMA-SiO<sub>2</sub> film onto Au/Si substrate. The average thickness of the dielectric layer is ~440 nm

between 5 and 1,000 Hz [17, 18], this fact is related to the carrier lifetime and thermal generation rate in the silicon substrate. As consequence, the C–V curves for MIS devices measured at high frequencies do not show the increase of capacitance in strong inversion. For these devices the dielectric constant and capacitance density results are also shown in Figs. 5 and 6. The values of  $\kappa_i$  were calculated from the maximum capacitance, resulting in values in the range of 10–16 for the frequency range between 1 and 1,000 kHz. Clearly the capacitance is frequency dependent (consequently  $\kappa_i$ ), it decreases gradually with increasing frequency, as expected in an organic system. This is because at a sufficiently high frequency the dipolar moment orientation is limited and the interface traps do not respond, therefore their contribution to the capacitance and the dielectric constant diminishes. The dielectric constants in Fig. 6 were estimated at 1, 10, 100, and 1,000 kHz with the C–V measurements using MIM and MIS structures. The dispersion of the  $\kappa$  values at low frequencies is considerably larger than at high frequencies, were the estimated  $\kappa$  data show a similar trend and good agreement between the two different structures employed. The average  $\kappa$  value estimated at 1 MHz was ~9.5.

It is well known that the dielectric permittivity of a material is proportional to its electronic polarization. Materials with polar groups (i.e. C=O) have large dielectric constants due to the orientation of their electrical dipoles in an applied electric field. Among the organic functional groups, –OH has the highest molar polarization [19]. Polar polymers have a tendency to retain moisture, which further increases their dielectric constants. Also, it is known that for materials with a large number of carbon atoms the polarizability increases in the order of single, double and triple bonds due to the enlarged mobility of the  $\pi$  electrons [20]. The total polarization is the result of the contribution

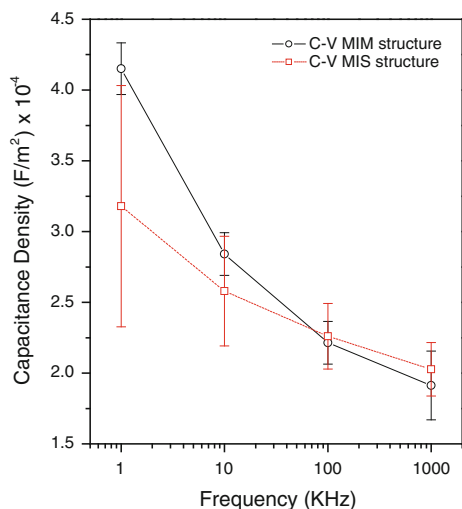


**Fig. 5** Frequency dispersion of the capacitance per unit area by C–V measurements

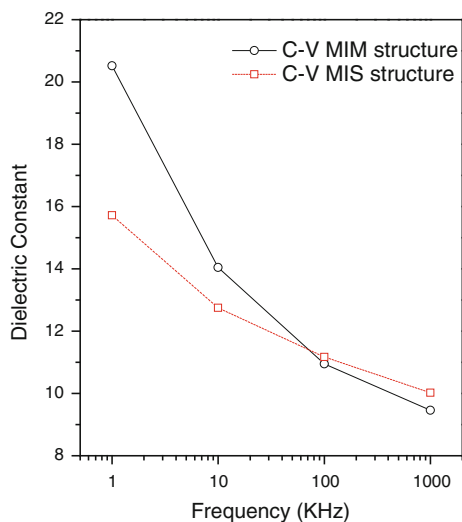


**Fig. 6** Comparison of the dielectric constant values calculated using MIM and MIS stack structures at different frequencies for PMMA-SiO<sub>2</sub> hybrid material

of different factors: electronic, atomic or ionic, and orientation responses of the material, with at least one of these polarization modes exhibited in dielectric materials. At high frequencies the electronic responses dominate, while ionic and orientational contributions are important at low frequencies. Thus, the explanation of the large dielectric constant in our hybrid films must take into account all of these issues. The PMMA-SiO<sub>2</sub> samples exhibit greater dielectric constant than the  $\kappa$  values typically reported for PMMA ( $\kappa = 3.2$  at 1 MHz) [21] and for SiO<sub>2</sub> ( $\kappa = 3.9$  at 1 MHz) [22]. This variation could be attributed to the presence of highly polarizable bonds contained in the PMMA-SiO<sub>2</sub> hybrid films, such as C–O–C, C=C, C=O and O–H bonds, as was determined from the FTIR results. We

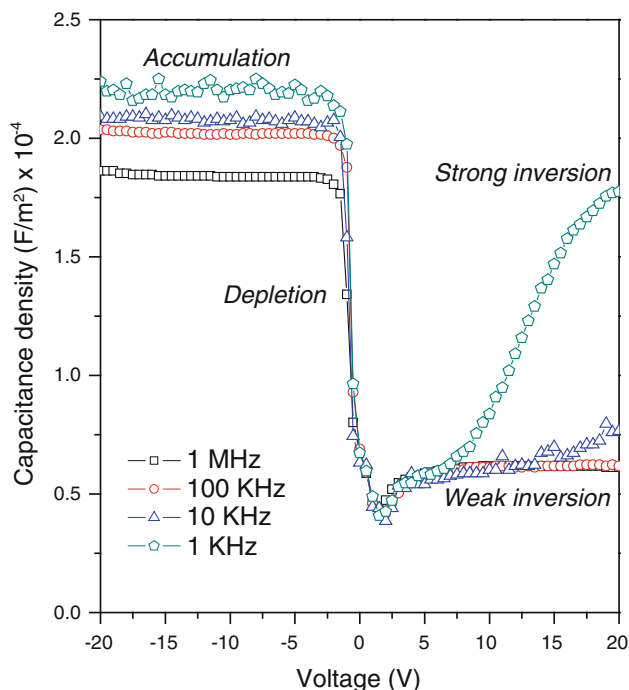


**Fig. 7** C–V characteristics curves for MIS devices show the typical behavior at high and low frequencies

believe that the dielectric behavior of the PMMA-SiO<sub>2</sub> material might be dominated by the hydroxyl groups that remain in the hybrid films, even after the long heat treatment. Similar dielectric constant behavior was seen in previous work by Na et al. [21] for cyanoethyl pullulan (CEP) material, in Aluminum/CEP/p-Si MIS structures, where the reported high dielectric constant values ( $\kappa \sim 16$  at 1 MHz) were associated to polar groups like –C  $\equiv$  N and C–O–C– contained in the CEP films.

A more detailed analysis was carried out using MIS capacitors, which are used to understand the quality of PMMA-SiO<sub>2</sub>/Si interface. Figure 8a shows the C–V behavior for a MIS configuration at 1 MHz frequency. The curves were recorded scanning forward (from negative to positive) and backward voltages, at room temperature. The doping density of the semiconductor ( $N_A = 3.8 \times 10^{14}/\text{cm}^3$ ) was determined from the slope of  $1/C^2$ –V curve. The corresponding flat band voltage ( $V_{FB}$ ) was determined from the experimental C–V plots with the calculated flat band capacitance ( $C_{FB}$ ) [16]. The  $V_{FB}$  for an ideal MIS capacitor is assumed to be zero. For our MIS devices  $V_{FB}$  was shifted lightly negative,  $V_{FB} = -0.38$  V, which indicates that the polarity of the charges is positive [23]. The curves show low hysteresis ( $\Delta V_{FB} = 0.04$  V) indicative of the presence of traps close to the PMMA-SiO<sub>2</sub>/Si interface. Using the  $V_{FB}$  value, the oxide trapped charge density ( $N_{ox}$ ) was estimated as  $7.03 \times 10^{10} \text{ cm}^{-2}$ . The order of magnitude of this oxide charge density calculated, is comparable

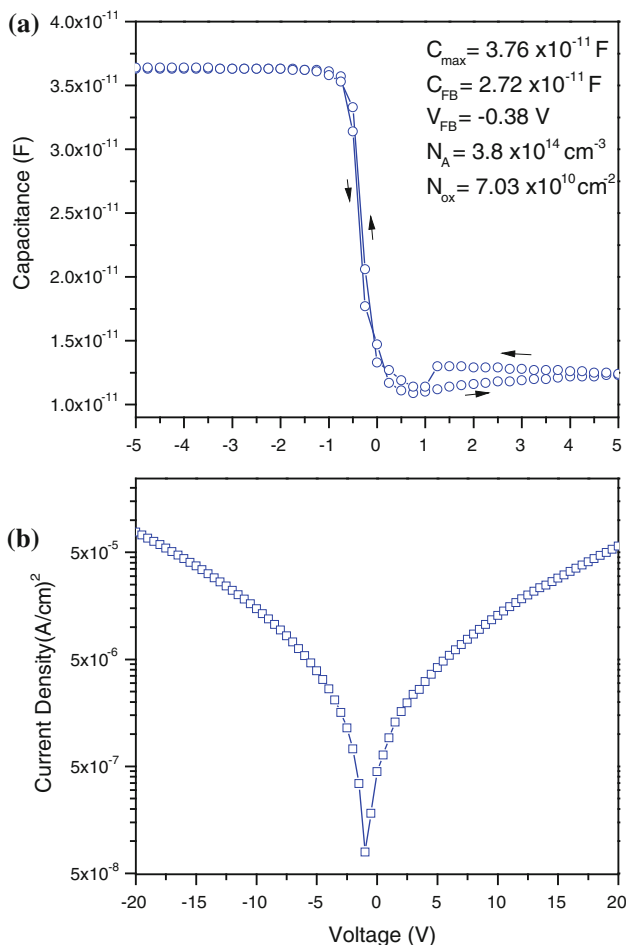


**Fig. 8** **a**  $C$ - $V$  curve for MIS devices at 1 MHz frequency and **b**  $I$ - $V$  characteristic

to those of standard  $\text{SiO}_2/\text{Si}$  structures ( $\sim 10^{10} \text{ cm}^{-2}$ ). Figure 8b shows the  $I$ - $V$  characteristic curve for gate voltages from  $-20$  to  $+20$  V, the leakage current density is ranging from  $5 \times 10^{-8}$  to  $5 \times 10^{-6} \text{ A/cm}^2$  for values between 0 and 10 V. This current density is higher than the characteristics leakage current values reported for PMMA ( $10^{-8} \text{ A/cm}^2$ ) [20], which could be explained by the presence of remainders O-H groups in the hybrid films. Further studies are considered to explain the electrical behavior with the effect of processing temperature, in particular at temperatures  $> 90^\circ \text{C}$  to reduce the content of hydroxyl groups in the films. The reduction of the hydroxyl groups and the concomitant reduction of the leakage current is a key point to allow the PMMA- $\text{SiO}_2$  hybrid material plays the role of gate dielectric in electronic devices.

#### 4 Conclusions

In this work, we have successfully implemented hybrid PMMA- $\text{SiO}_2$  films as dielectric in MIM and MIS stacks.

Through its  $C$ - $V$  electrical characterization, PMMA- $\text{SiO}_2$  films show higher dielectric constant ( $\kappa \sim 9.5$  at 1 MHz) than thermally grown  $\text{SiO}_2$  and pure PMMA materials. Furthermore, the density of charge in the films ( $\sim 10^{10} \text{ cm}^{-2}$ ) is comparable to those usually obtained for MIS structures with  $\text{SiO}_2$  as the gate dielectric. PMMA- $\text{SiO}_2$  organic-inorganic films offer attractive opportunities for electronic applications, due to the combined functional features of both organic and inorganic components in a single molecular scale hybrid dielectric material with good electrical properties, compatible with existing processing technologies. Furthermore, this material is fully compatible for applications in flexible electronics.

**Acknowledgments** This work was partially supported by CONA-CyT. Technical assistance of J.E. Urbina and C.A. Avila-Herrera is also gratefully acknowledged.

#### References

- Wallace MR, Wilk GD (2003) High- $\kappa$  dielectric materials for microelectronics. *Crit Rev Solid State Mater Sci* 28:231–285
- Puigdollers J, Voz C, Orpella A, Quidant R, Martín I, Vetter M, Alcubilla R (2004) Pentacene thin-film transistors with polymeric gate dielectric. *Org Electron* 5:67–71
- Almaral-Sánchez JL, Rubio E, Mendoza-Galván A, Ramírez-Bon R (2005) Red colored transparent PMMA- $\text{SiO}_2$  hybrid films. *J Phys Chem Solids* 66:1660–1667
- Alvarado-Rivera J, Muñoz-Saldaña J, Castro-Beltrán A, Quintero-Armenta JM, Almaral-Sánchez JL, Ramírez-Bon R (2007) Hardness and wearing properties of  $\text{SiO}_2$ -PMMA hybrid coatings reinforced with  $\text{Al}_2\text{O}_3$  nanowhiskers. *Phys Stat Sol* 11:4254–4259
- Wen J, Wilkes GL (1996) Organic/Inorganic hybrid network materials by the sol-gel approach. *Chem Mater* 8:1667–1681
- Rubio E, Almaral J, Ramírez-Bon R, Castaño V, Rodríguez V (2005) Organic-inorganic hybrid coating (poly(methyl methacrylate)/monodisperse silica). *Opt Mat* 27:1266–1269
- Morales-Acosta MD, Quevedo-Lopez MA, Alsharef HN, Gnade B, Ramírez-Bon R (2010) Dielectric properties of PMMA- $\text{SiO}_2$  hybrid films. *Mater Sci Forum* 644:25–28
- Almeida RM, Pantano CG (1990) Vibrational spectra and structure of silica gel films spun on c-Si substrates. *SPIE-Sol-Gel Optics* 1328:329–337
- Medda SK, Kundu D, De G (2003) Inorganic-organic hybrid coatings on polycarbonate: Spectroscopic studies on the simultaneous polymerizations of methacrylate and silica networks. *J Non-Cryst Solids* 318:149–156
- Fidalgo A, Ilharco LM (2001) The defect structure of sol-gel derived silica/polytetrahydrofuran hybrid films by FTIR. *J Non-Cryst Solids* 283:144–154
- Innocenzi P (2003) Infrared spectroscopy of sol-gel derived silica-based films: a spectra-microstructure overview. *J Non-Cryst Solids* 316:309–319
- Sassi Z, Bureau JC, Bakkali A (2001) Structural characterization of the organic/inorganic networks in the hybrid material (TMOS-TMSM-MMA). *Vib Spectrosc* 28:251–262
- Sassi Z, Bureau JC, Bakkali A (2002) Spectroscopic study of TMOS-TMSM-MMA gels previously identification of the networks inside the hybrid material. *Vib Spectrosc* 28:299–318

14. Han YH, Taylor A, Mantle MD, Knowles KM (2007) Sol-gel derived organic-inorganic hybrid materials. *J Non-Cryst Solids* 353:313–320
15. Oliver WC, Pharr GM (1992) An improved technique for determining hardness and elastic modulus using load and displacement sensing indentation experiments. *J Mater Res* 7:1564–1583
16. Schroder DK (2006) *Semiconductor material and device characterization*, 3rd edn. Wiley, New Jersey
17. Hofstein SR, Warfield G (1965) Physical limitation on the frequency response of a semiconductor surface inversion layer. *Solid-State Electron* 8:321–341
18. Grove AS, Deal BE, Snow EH, Sah CT (1965) Investigation of thermally oxidized silicon surfaces using metal-oxide-semiconductor structures. *Solid-State Electron* 8:145–163
19. Ogura I (1999) In: Nalwa HS (ed) *Handbook of low and high dielectric constant materials and their applications*, vol I—materials and processing. Academic Press, Boston
20. Ho PS, Liu J, Morgen M, Kiene M, Zhao JH (2003) In: Murarka SP, Eizenberg M, Sinha AK (eds) *Interlayer dielectrics for semiconductor technologies*. Elsevier Inc, London
21. Na M, Rhee SW (2006) Electronic characterization of Al/PMMA[poly(methyl methacrylate)]/p-Si and Al/CEP(cyanoethyl pullulan)/p-Si structures. *Org Electron* 7:205–212
22. Sze SM, Ng KwokK (2007) *Physics of semiconductor devices*, 3rd edn. Wiley, New Jersey
23. Lee YK, Murarka SP (1999) Characterization of charges in fluorinated polyimide film with different thermal history by using capacitance-voltage methods. *Mater Res Bull* 34:869–876